18th IFHTSE CONGRESS
International Federation for Heat Treatment and Surface Engineering
IFHTSE
ANAIS
PROCEEDINGS
ISSN 1516-392X

INFLUENCE OF CUTTING SPEED ON THE SURFACE INTEGRITY OF AISI 304L AUSTENITIC STAINLESS STEEL PARTS[1]

Thompson Júnior Ávila Reis[2]
José Rubens Gonçalves Carneiro[3]
José Mário Carneiro Vilela[4]
Margareth Spangler Andrade[4]

Abstract
The present study aimed to investigate the influence of cutting speeds on the surface integrity of AISI 304L austenitic stainless steel parts. The samples were annealed and underwent mechanical turning at diverse cutting speeds, maintaining set levels for all other machining parameters. Optical microscopic analyses, as well as Scanning Probe Microscopy (SPM), were carried out in cross-sections of the samples to verify the occurrence of phase transformations, such as deformation induced martensite α'. Microhardness measurements were taken along the region affected by machining in an attempt to verify changes in the mechanical properties. The results indicate growing strain hardening due to an increase in the cutting speed and the presence of martensite α' in certain sample regions.
Key words: Austenitic stainless steel**;** Strain-induced martensite; Cutting speed; Surface integrity; Microhardness; Scanning probe microscopy (SPM).

INFLUÊNCIA DA VELOCIDADED DE NA INTEGRIDADE SUPERFICIAL DE PEÇAS DE AÇO INOXIDÁVEL AUSTENÍTICO AISI 304L

Resumo
O presente estudo teve como objetivo investigar a influência da velocidade de corte na integridade superficial de peças em aço inoxidável austenítico AISI 304L. As amostras foram recozidas e submetidas ao torneamento em diversas velocidades de corte, mantendo fixos todos os outros parâmetros de usinagem. Análises de microscopia ótica, bem como microscopia de varredura por sonda foram realizadas através da seção transversal das amostras para verificar a ocorrência de transformação de fase, como martensita α' induzida por deformação. Medições de microdureza foram feitas ao longo da região afetada pela usinagem, com intuito de verificar alterações nas propriedades mecânicas. Os resultados indicam encruamento crescente em função do aumento da velocidade de corte e a presença de martensita α' em algumas regiões das amostras.
Palavras-chave: Aço inoxidável austenítico; Martensita induzida por deformação; Velocidade de corte; Integridade superficial; Microdureza; Microscopia de varredura por sonda (MVS).

[1] *Technical contribution to the 18th IFHTSE Congress - International Federation for Heat Treatment and Surface Engineering, 2010 July 26-30th, Rio de Janeiro, RJ, Brazil.*
[2] *Specialist in Metallurgical Process of Manufacture – Universidade Presidente Antônio Carlos (UNIPAC)/ Pontifícia Universidade Católica de Minas Gerais(PUC Minas.*
[3] *Dr., Mechanical Department - Pontifícia Universidade Católica de Minas Gerais/PUC Minas.*
[4] *Dr., Metallurgy Department – Fundação Centro Tecnolólogico de Minas Gerais – CETEC.*

1 INTRODUCTION

Manufacturing processes by machining differ from all others in a number of aspects. One such aspect is related to the good surface quality and high dimensional precision attributed to the final product. Machining is nearly always applied at some stage of the manufacturing process of approximately 80% of all parts classified as finished or ready-for-use products.[1]

In machining, the form, dimension, and finishing of the product are obtained by means of localized extraction of the material through respective movements between the part and the cutting tool. This is different from the mechanical forming processes where the form, dimension, and finishing of the part are obtained via plastic deformation.[1-3]

The machining of a great majority of parts is carried out in two distinct stages. The first stage, known as rough machining, is aimed at removing the largest amount of material possible per unit of time. This is carried out through the use of larger advances (f), associated with cutting depths (a_p), which are also high; however, the cutting speeds (v_c) are considerably lower when compared to those used in the finishing stage. The purpose of the finishing stage is to provide the part with surface quality and the desired dimensions according to that specified in the project. To attain these goals, smaller advances and cutting depths are used, whereas the cutting speed tends to be greater. The combination of the cutting speed and the advance, as described for the finishing stage, allows for favorable conditions so as to obtain a good surface quality for the part. The smaller depth of the cut minimizes elastic deformities of the part and contributes, together with the stiffness of the equipment, to obtaining precise dimensions. There is also a great concern regarding the heat dissipated in this stage; the fraction dissipated by the part, which can lead to such dilation that one cannot guarantee dimensional precision; and the fraction of heat dissipated by the tool, which can lead to its premature breakdown.[2,3]

Machining for finishing is less aggressive on the material of the part when compared to rough machining; however, high rates of deformation, due to high cutting speeds, concentrated in a very small area are characteristic features of this phase and may well contribute to the occurrence of changes in its surface layer. Such changes become permanent due to the fact that this is the final manufacturing stage to which the material is submitted when being transformed into a ready-for-use product.

Surface integrity treats the study and control of diverse changes produced in the surface layer of the machined products. These changes may be metallurgical, such as phase transformations; mechanical, when the mechanical properties are changed; or chemical, if contamination of the part occur.[4] Many studies related to the behavior of the materials when submitted to a machining process reveal the importance of clarifying these phenomena, given that the changes in the microstructure and material properties can greatly influence the service life of the manufactured product.

Residual tensions, which directly influence in the resistance of the component when undergoing cyclical stress, were studied by Gravalos (2008) in superaustenitic stainless steel and related to machining parameters. Gravalos demonstrated in his work that when the cutting speed for finishing is increased, the residual tension is reduced; the exit angle of the tool and the depth of the cut do not influence this parameter. Within all conditions studied by Gravalos, residual tensions were of traction.[5] Pitella also investigated residual tension of machining conditions in a C45 PBK carbon steel. In his work, milling conditions and normal and severe grinding

were studied and associated with residual tensions. The results indicated compressive residual tensions when the conditions were normal and residual tensions of traction when the machining conditions were severe.[6]

Gravalos also studied changes in the mechanical properties of some superaustenitic stainless steels through microhardness profiles measurements in the layer affected by machining and demonstrated that a layer with increased hardness did in fact exist, indicating the strain hardening of the material.[5,7]

Other studies have also investigated the machining parameters as regards the resistance of the material to fatigue. Lopes investigated the possible relations of the machining parameters with the behavior of the AISI 4140 carbon steel under fatigue. His work demonstrated that the increase in cutting speed causes an increase in the resistance of the material to fatigue in an almost linear manner, whereas the advance, when increased, presents a significantly negative effect on the resistance of the component to fatigue.[8]

The present study aimed to complement the already existing knowledge on the behavior of materials when machined, especially that which refers to surface integrity. These findings are innovative and of extreme relevance as they show the possible metallurgical transformations which occur on the surface of the material and which result from machining conditions. To reach such a conclusion, an austenitic stainless steel was chosen. These steels include a distinct group among all stainless steels, as they possess face centered cubic structures and the austenite remains stable at room temperature.[9] The austenitic stainless steels can react in a unique manner, forming deformation induced martensite when the chemical composition, the temperature conditions, and the amount and rates of deformation are favorable.[9,10] The deformation induced martensite phases can be reverted to austenite through thermal treatments at temperatures of approximately 200ºC for ε martensite and at temperatures of 600-800ºC for α'martensita.[11,12] Microhardness profiles, optical microscopy and scanning probe microscopy (SPM) were performed in samples machined in different conditions.

2 MATERIAL AND METHODS

2.1 Materials

The material analyzed was an AISI 304L austenitic stainless steel acquired in round bars of 15.90 mm in diameter with a drawn finishing. Before machining, the steel was thermally treated by annealing at 1000ºC for 3 hours to recrystallize the structure that was strain hardened by drawing. Table 1 presents the chemical composition of the alloy.

Table 1. Chemical composition of the steel studied (wt%)

	C	Mn	Si	Cr	Ni	P	S
AISI 304L	0.024	1.650	0.391	17.98	10.08	0.029	0.010

2.2 Machining Equipment and Parameters

The samples were machined in two different sets of equipment due to the rotation limits of one of these. The CNC lathe, from the Romi 30D Centure model, was used to machine the samples at a rotation of less than or equal to 4,000 RPM

and a of Romi lathe center line E, model 280, was used to machine the samples at a rotation of above 4,000 RPM.

The selected cutting tool was the ISO TNMG 160404 hard metal insert with a triple coating of TiCN + Al_2O_3 + HfN produced by Walter and the support used to secure the hard metal insert carbide was the ISO DTGNR 2525 M16. This support holds the insert carbide at a position angle (χ_r) of 93º, a rest angle (θ) of 6º, and an exit angle (α) of 13º.

All of the samples were cooled during machining with a Blascut 2000 cutting fluid produced by Blaser. Its concentration in water was of 8%.

The cutting advance and the cutting depth were set at 0.12 mm/rev and 1.00 mm, respectively. These conditions represent the maximum limits suggested by the manufacturer of the selected metallic insert. The only machining parameter that varied was the cutting speed.

The diameter of the samples after machining was of 13.9 mm. Through the machined diameter, the ideal cutting speed of 292 m/min on the tool's tip to advance the selected cut could be determined according to manufacturer instructions. This result indicated a considerably high rotation (approximately 6700 RPM) due to the fact that the diameter of the samples was small and the cutting speed was relatively high. This fact represented a limitation for the development of the work due to the difficulty of the availability of the equipment with the capacity to perform such a rotation. The present study analyzed machined samples at four different cutting speeds, each below the ideal cutting speed suggested by the manufacturer. Table 2 presents the rotations and the cutting speeds used.

Table 2. Rotations and cutting speeds used in the experiment

Sample	Rotation (RPM)	Cutting Speed (m/min)
1	3000	130
2	4000	175
3	5000	220
4	6000	260

2.3 Methodology of Analysis

2.3.1 Preparation of the samples

To perform the microhardness assays, the samples were extracted in a direction that was cross-sectional to the drawing, considering that the material analyzed possesses a relatively large quantity of inclusions of manganese sulfides in its microstructure. The stretched form of this second phase in the direction of the drawing makes the measurement of the microhardness difficult in samples that have been removed in a longitudinal direction, as this is a softer phase and influences the measurement when indentation occurs. In the cross-sectional direction, the manganese sulfides are distributed as much smaller points than the indentations and do not produce such an intense influence on the microhardness results.

The samples were sanded and polished with a 1µm cloth and later polished with an OP-S colloidal solution for three minutes. This was performed so as to obtain samples with the flattest surface possible and free of deformation induced martensite from the polishing. For the SPM analyses, the samples were prepared in the same.

For optical microscopic analyses, the samples were etched with aqua regia for 15 seconds, or Vilela for 90 seconds or with Beraha, with an exposure time of four seconds, always after having been polished in an OP-S solution.

2.3.2 Microhardness

The purpose of carrying out microhardness assays is to verify changes in the mechanical properties of the material in the surface layer affected by deformation produced by machining. The Knoop measurement hardness test was selected as the indentation produced presented one diagonal that was many times greater than the other, allowing the measurements to be taken as near as possible to the outer portion when carried out parallel to the indentation. The load chosen was of 50gf. Greater loads allow for more precise measurements, but as this material was a relatively soft austenitic stainless steel, greater loads than these produced indentations of such a magnitude that measurements become nearly impossible. The measurements were taken up to a distance of 0.3 mm from the sample border, since it could be observed that, up to this distance, the hardness had already reached the level of the annealed material. The microhardness profiles were obtained by determining the average of the four measurements taken at each surface distance.

2.3.3 Scanning probe microscopy (SPM)

Scanning Probe Microscopy (SPM) is a technique which allows for the realization of diverse types of analysis. Generically speaking, the technique consists of scanning a region of the sample using a very fine probe. A laser is placed on this probe, which is then reflected onto a photo-sensor. The probe touches the surface and is pulled over it to carry out the scanning process. This movement causes the probe to oscillate from top to bottom, as for example, with the topography of the sample. The oscillation of the probe makes it so that the laser reflected onto the photo-sensor also oscillates. A computer collects these data and reproduces the topographical images of the region scanned by the probe. In this case, the technique is called atomic force microscopy (AFM), as it acts on the weak forces of the material

The SPM technique allows, in addition to the reproduction of the topography of the material, the analysis of the magnetic potentials, acting on the strong forces of the materials. In this case, the scanner is magnetized and will interact by being attracted or repelled by the material when displaced to a nanometric surface distance of the material. The result is an image that presents the various magnetic potentials of the surface in a variety of tones. This second technique is known as magnetic force microscopy (MFM).

The use of MFM provided a great contribution to this work, as it allowed for the identification of magnetic regions in a non-magnetic matrix. As has already been reported, austenitic stainless steels are paramagnetic, whereas the deformation induced martensita α' is ferromagnetic.

3 RESULTS AND DISCUSSION

3.1 Microhardness

Figure 1 presents the microhardness profiles of the four machined samples together with the results obtained in the as drawn and annealed samples.

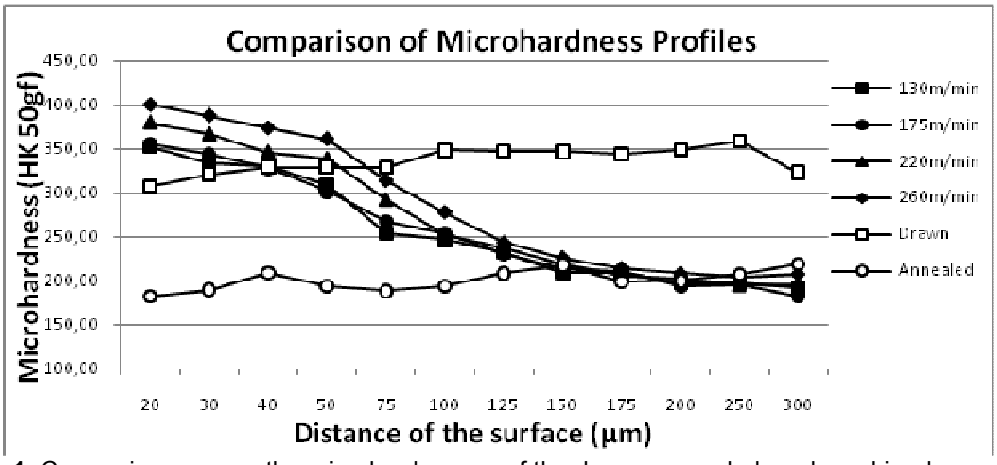

Figure 1. Comparison among the microhardnesses of the drawn, annealed, and machined samples.

The information presented in Figure 1 indicates that upon comparing the increase in hardness of the machined samples with the hardness of the annealed sample a significant increase could be observed, especially up to a depth of 50µm . However, when comparing the same information from the machined sample with the results obtained from the measurements of the drawn sample, it could be observed that only the samples that were machined at cutting speeds of 220m/min and 260m/min presented greater hardnesses than those of the annealed sample. Nevertheless, for the sample machined at 220m/min, these hardnesses were only found to be greater than those of the drawn material in the most superficial layer, with a depth of less than 40µm. The sample that presented the most relevant increase in hardness, as compared to that obtained in the drawn sample, was the machined at a cutting speed of 260m/min, reaching 400HK at a depth of 20µm, maintaining a hardness of greater than 350HK up to depths of 50µm. The aim of the comparison of the results of the machined with the drawn samples is due to the fact that this is the condition in which the material can be purchased on the market.

Figure 2 presents the average and the highest hardness obtained for the most relevant depths in all of the machined, annealed, and drawn samples. Considering the configuration of the information in this figure, it could be observed that for all samples the hardness fell as the depth increased. Another fact that can be analyzed is that only a small difference could be observed between the greater hardnesses and the average hardnesses in all cases, which indicates that the measurements were rarely influenced by the different phase present in the material, such as manganese sulfide. Within this figure, it can also be observed that there are practically no differences between the machined sample data at 130 and 175m/min. An increase in the average hardness and a greater hardness could be observed at depths of 20 and 50µm, but only for samples machined at 220m/min. The hardness increased at a depth of 100µm only for the sample machined at a cutting speed of slightly less than 260m/min. At depths in the order of 200µm, the hardness of the machined samples was equal to the hardness of the annealed sample.

As regards the drawn sample, this figure illustrates that both the average and greater hardnesses increased with depth, reaching their highest values at a depth of 200µm. In this sample, no significant difference between the average and greater hardnesses could be observed.

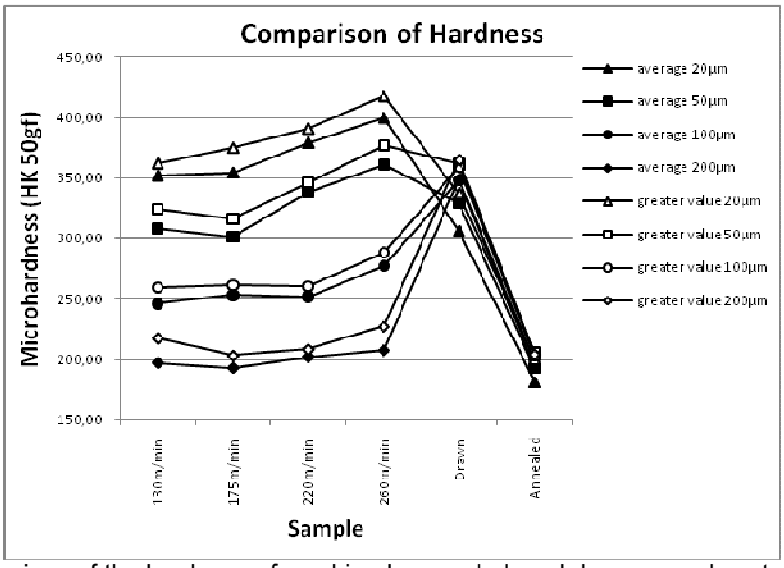

Figure 2. Comparison of the hardness of machined, annealed, and drawn samples at selected depths.

3.2 Scanning Probe Microscopy

Figures 3 and 4 illustrate magnetic particles observed MFM in the regions affected by the machining of the sample machined at 175m/min. Only in this sample it was possible to observe magnetic particles, even if in a small quantity, which indicates that these are particles of deformation induced martensite α'.

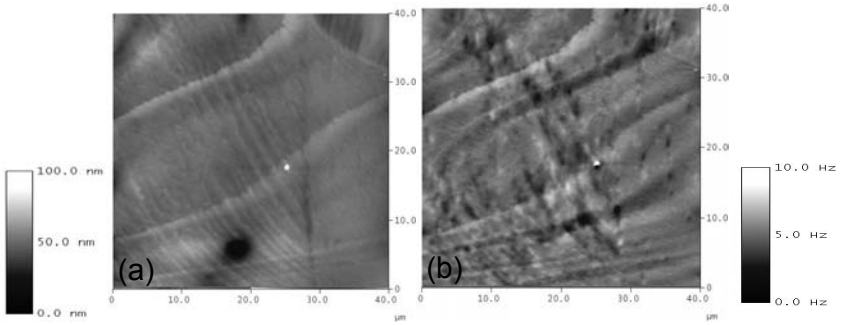

Figure 3. Images (a) topographic (AFM) and (b) magnetic (MFM) of the region affected machining of the sample machined at 175m/min. Dark spots in the (b) image indicate magnetic particles.

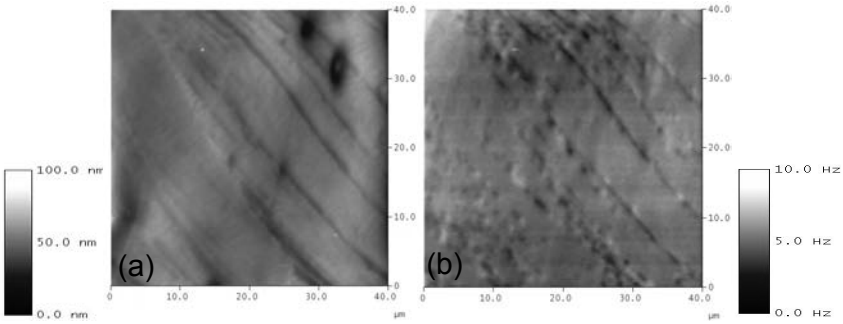

Figure 4. Images (a) topographic (AFM) and (b) magnetic (MFM) of a region affected machining of the sample machined at 175m/min. Dark spots in the (b) image indicate magnetic particles.

The non-formation of martensite α' in the majority of the samples is related to the chemical composition, elements which stabilize the martensite at high-grade levels, as is the case with Nickel. The temperature that the samples reach when machined and the rate of deformation to which each of the samples was submitted are also important factors. As the chemical composition is the same for all the samples, the higher temperatures reached in the samples machined at higher speeds most likely inhibited the formation of martensite. The non-formation of martensite in the sample machined at a slower speed may well be related to the lesser rate of deformation to which the material was submitted.

In the two images illustrated in Figures 3 and 4, the presence of "deformation bands", regions with a lower topography than the rest of the matrix, could be observed. In Figures 3a and 4a, these bands appear as gross parallel lines that partially cut the grains of the material. In the magnetic images, Figures 3b and 4b, the presence of a magnetic phase with a similar morphology could be observed at points located sequentially along the bands viewed in the topographical image. The already known strain hardening conditions of the region affected by machining, associated with the presence of a magnetic phase in the same region, indicate that this is martensite α'.

In the sample machined at 260m/min, the presence of deformation bands in some regions could be confirmed; however, it was impossible to affirm the presence of martensite α' due to technical issues that occurred during the period in which they were analyzed, in which only topographical images of this sample could be taken. Figure 5 presents the presence of deformation bands at two different points in the region affected by machining in the sample machined at 260m/min.

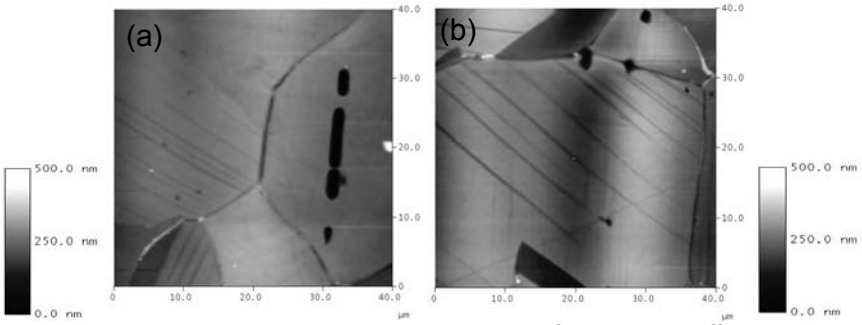

Figure 5. Topographic images (AFM) at two distinct points of the region affected by machining in a sample machined at 260m/min, indicating the presence of deformation bands.

This sample was extracted in a direction which was longitudinal to the drawing. Due to the manner of preparation of the sample, the topography can be seen in a larger scale in the z direction (in the order of 500nm) than that of the polished samples in OP-S solution, whose z scale was approximately 50 to 200nm. It was not observed either the deformation bands or the presence of the magnetic phase, martensite α', in the samples machined at cutting speeds of 130 and 220m/min using SPM techniques. Figures 6 and 7 illustrate: topographical images, 6a and 7a; and magnetic images, 6b and 7b, performed on the samples machined at 130 and 220m/min, respectively. Both the samples were extracted in a direction that was cross-sectional to the drawing and were polished in an OP-S solution.

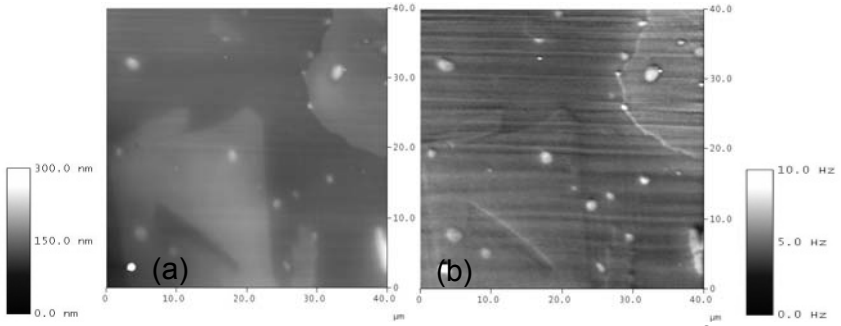

Figure 6. Images (a) topographical (AFM) and (b) magnetic (MFM) of the region affected by machining of the samples machined at 130m/min. The (b) image shows no magnetic particles.

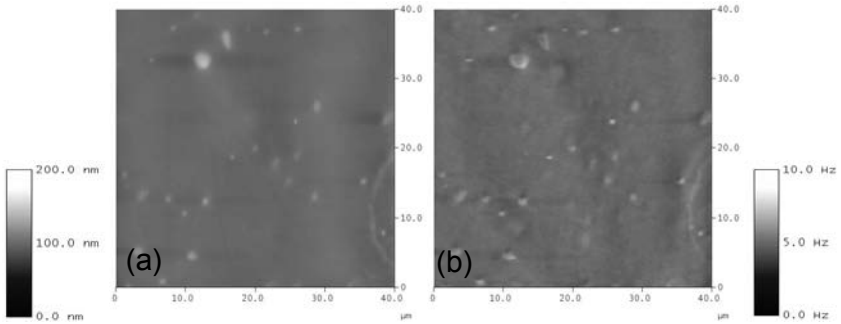

Figure 7. Images (a) topographical (AFM) and (b) magnetic (MFM) of the region affected by machining of the samples machined at 220m/min. The (b) image shows no magnetic particles.

It is important to note that the points that appear to be topographically higher in both Figures 6a and 7a characterize impurity remaining from the OP-S polishing process.

3.3 Optical Microscopy

The presence of deformation bands was also observed by the optical microscopic analyses in all machined samples. The results of the microhardness assay confirmed a similar thickness for the affected layers by machining in all the samples observed at the optical microscope. This fact can be confirmed by comparing the results illustrated in Figure 1.

Figure 8 presents images of the region affected by machining in all machined samples.

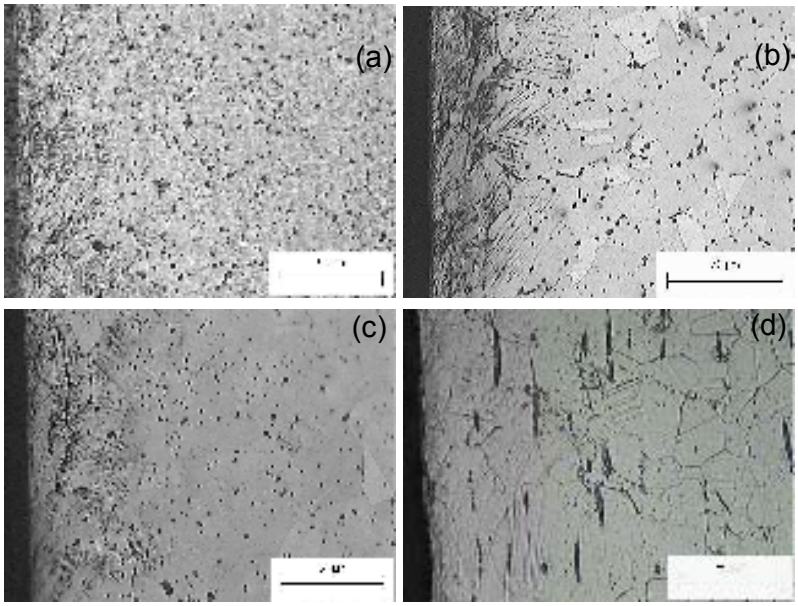

Figure 8. Deformation bands in the surface layer of the machined samples at (a) 130m/min etched with Beraha, (b) 175m/min etched Vilela, (c) 220m/min etched Vilela, and (d) 260m/min electrolytically polished.

4 CONCLUSIONS

- All samples underwent changes in the mechanical properties with increase in hardness in the surface layer affected by machining due to the increase in cutting speed. The hardness at a depth of 20μm increased from 200HK (hardness of the annealed material) to values in the order of 400HK;
- The hardness of the samples machined at a cutting speed of less than 175m/min increased from 200HK to 350HK at a depth of 20μm, reaching the hardness values of the drawn material;
- The hardness of the samples machined at a cutting speed of greater than 175m/min increased from 200HK to 380HK (v_c = 220m/min) and 400HK (v_c = 260m/min) at a depth of 20μm, increasing beyond the hardness values of the drawn material by 8.6% and 14.3%, respectively;
- The strain hardening maintained the hardness at greater levels, with only slight reductions in function to the cutting speed, at depths of up to around 50 to 75μm. The reduction in the hardness was more accentuated, reaching the values of the annealed steel, at depths of around 150 to 175μm, also depending on the cutting speed;
- The SPM analyses indicated the formation of α' strain induced martensite in small quantities in the layer affected by machining only in the sample machined at a cutting speed of 175m/min. The chemical composition, the process temperature, and the rate of deformation are determining factors for the transformation of deformation induced martensite.
- The presence of "deformation bands" could be observed in the samples by optical and atomic force microscopy.

Acknowledgements

T. J. A. R. and J. R. G. C. thank Pontifícia Universidade Católica for their support. J. M. C. V. and M. S. A. thank FAPEMIG for their financial support and scholarships.

REFERENCES

1 DIETER, G. E. Mechanical metallurgy SI metric edition. Adapted for David Bacon. 3. ed. New York: McGraw-Hill Book, 1988.
2 DINIZ, A. E.; MARCONDES, F. C.; COPPINI, N. L. Tecnologia da Usinagem dos Materiais. 5. ed. São Paulo: Artliber Editora, 2006.
3 FERRARESI, D. Fundamentos da Usinagem dos Metais. São Paulo: Edgard Blücher, 1970.
4 ASM Handbook: *Machining Processes.* v. 16. ASM International, 1992.
5 GRAVALOS, M. T. Efeitos da Usinagem na Integridade Superficial de um Aço Inoxidável Superaustenítico. Campinas, Faculdade de Engenharia Mecânica, Universidade Estadual de Campinas, Dissertation of Master´s Degree, 2008.
6 PITELLA, R. M.: Determinação de Tensões Residuais em Aço C45 PBK em Condições Limites de Usinagem. Curitiba, Departamento de Engenharia Mecânica, Universidade Federal do Paraná, Dissertation of Master´s Degree, 2003.
7 GRAVALOS, M. T.; MARTINS, M.; DINIZ. A. E.; MEI. P. R. Efeito da Usinagem na Estrutura e Propriedades Mecânicas do Aço Superaustenítico ASTM A351 CN3MN. REM magazine, Brazil, 2006, pp. 83–88.
8 LOPES, K. S. S. Influência dos Parâmetros de Usinagem na Resistência à Fadiga de Aços AISI 4140. Belo Horizonte, PUC-Minas, Dissertation of Master's Degree, 2006.
9 PADILHA, A. F.; GUEDES, L. G. Aços inoxidáveis austeníticos microestrutura e propriedades. Curitiba: Hemus, 2004.
10 KRAUSS, G. Steels: heat treatment and processing principals. 5. ed. Evergreen: Materials Park, 1997.
11 SANTOS, T. F. A.; ANDRADE, M. S. Avaliação Dilatométrica da Reversão das Martensitas Induzidas por Deformação em um Aço Inoxidável Austenítico do Tipo ABNT 304. Revista Matéria v. 13 n. 4, Brazil, 2008, pp. 587–596.
12 SANTOS, T. F. A.; ANDRADE, M. S.; CASTRO, A. L. R. Efeito da Taxa de Aquecimento na Reversão da Martensita Induzida por Deformação em um Aço Inoxidável Austenítico do Tipo ABNT 304. Revista REM, Minas Gerais, Brazil, 2009, pp. 53–58.